JOURNAL OF ENGINEERING SCIENCES

Volume 8, Issue 1 (2021)

Demianenko M., Volf M., Pavlenko I., Liaposhchenko O. (2021). Experimental studies on oscillation modes of vibration separation devices. Journal of Engineering Sciences, Vol. 8(1), pp. D1–D9, doi: 10.21272/jes.2021.8(1).d1

Experimental Studies on Oscillation Modes of Vibration Separation Devices

Demianenko M.[1*[0000-0002-4258-0379]], Volf M.[2[0000-0002-2904-8994]],
Pavlenko I.[1[0000-0002-6136-1040]], Liaposhchenko O.[1[0000-0002-6657-7051]]

[1] Sumy State University, 2, Rymskogo-Korsakova St., 40007 Sumy, Ukraine;
[2] University of West Bohemia, 2738/8, Univerzitni St., 301 00 Pilsen, Czech Republic

Article info:
Paper received: February 2, 2020
The final version of the paper received: April 12, 2020
Paper accepted online: April 17, 2020

***Corresponding email:**
m.demianenko@omdm.sumdu.edu.ua

Abstract. Despite the rapid development of alternative energy sources, the role of hydrocarbons in the global fuel and energy balance remains significant. For their transportation and further processing, pre-processing is carried out using a set of equipment. In this case, the mandatory devices are separators. In terms of specific energy consumption and separation efficiency, methods based on the action of inertia forces are optimal. However, standard designs have common disadvantages. A method of dynamic separation is proposed to eliminate them. The proposed devices are automatic control systems. The object of regulation is hydraulic resistance, and elastic forces are the regulating actions. Aerohydroelastic phenomena accompany the operation of dynamic separation devices. Among them, the most interesting are flutter and buffeting. Oscillations of adjustable baffles accompany them. It is necessary to conduct a number of multifactorial experiments to determine the operating parameters of dynamic separation devices. In turn, physical experiments aim to identify patterns and features of processes occurring during vibration-inertial separation (i.e., the dependence of various parameters on velocity). Therefore, the article proposes a methodology for carrying our physical experiments on dynamic separation and a designed experimental setup for these studies. As a result, the operating modes of separation devices for different thicknesses of baffle elements were evaluated. Additionally, the dependences of the adjustable element's deflections and oscillation amplitudes on the gas flow velocity were determined for different operating modes of vibration separation devices.

Keywords: gas-liquid mixture, dynamic separation, deformable elements, oscillations, regression model.

1 Introduction

The role of oil and gas in the global fuel and energy balance is constantly growing. In 2018, oil and gas consumption was grown by 4.6 %, which accounted for half of the global increase in energy demand [1].

Notably, oil and natural gas extracted from the well are multiphase multicomponent mixtures. Mainly, the amount of droplet liquid in natural gas, consisting of mineralized water and gas condensate, is usually contained in the amount of 30–40 g/m^3, and sometimes even 200–800 g/m^3 [2]. Therefore, such gas-dispersed systems are processed before their further transportation and processing. Moisture separation improves the quality of the source product and ensures the reliability of compressor equipment for compression and pumping of gases. The presence of dripping liquids and mechanical impurities in the gas flow leads to emergencies and premature wear of the rotor necks and blades of compressors and superchargers [3]. The main technological methods of industrial gas preparation are separation, absorption purification, and stabilization. In this case, separation equipment is a mandatory one at industrial gas treatment plants [4].

The extracted oil contains formation water, associated gas, mineral salts, and mechanical impurities. Pure oil is the primary raw material for producing liquid energy, oils and lubricants, bitumen, and coke. For example, flooding crude oil with formation water and dissolved salts leads to a decrease in the quality of the oil itself and its products. [5].

Comprehensive oil preparation for transportation and further processing involves its degassing, dehydration, desalination, and stabilization. The degassing process begins immediately after the gas-liquid mixture enters the apparatus. Associated petroleum gas is usually released in quantities not sufficient for its transportation. Therefore, there is a need to dispose of it by burning it on a torch.

The use of associated petroleum gas as a fuel, which increases its energy efficiency, has become widespread. In the cases of the utilization of associated petroleum gas and its use as a fuel for more efficient combustion, dehydration is carried out to prevent the formation of crystal hydrates. Purification from heavy hydrocarbons prevents fluid blockages. The absence of hydrogen sulfide and carbon dioxide prevents corrosion on the equipment [6].

Therefore, before the transportation and further processing of natural gas and crude oil, the obligatory stage is separating the gas-liquid mixture. For this purpose, separators are used. Their operation is based on the balance of mass forces and aerodynamic drag forces.

2 Literature Review

A method of dynamic separation is proposed to extend the range of effective operation of separation devices designed to purify gas flows from liquid droplets (separation of gas-liquid mixture). According to this method, the gas stream containing the droplet liquid enters the separation channel, in which the elastic elements are cantilevered [7, 8]. These elements distort the flow of the mixture (Figure 1).

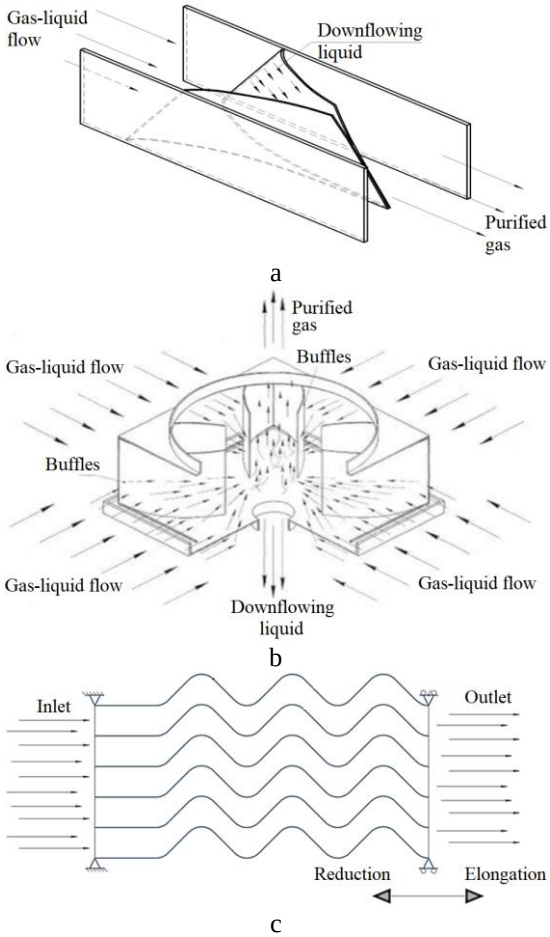

Figure 1 – Design schemes of separation devices

Under the action of inertia forces, the droplets contained in the gas deviate from the curved trajectory of the gas and settle on the walls, forming a film of liquid. Under dynamic pressure, the elastic elements change their configuration. This causes a change in flow parameters, and therefore, there are aeroelastic phenomena. This approach allows us to adjust the values of dynamic pressure and cross-sectional area automatically.

Figure 2 reflects the main differences in the operation of dynamic separation devices before the loss of static and dynamic stability compared with the traditional louver separation elements.

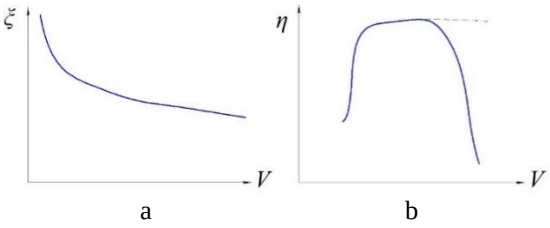

Figure 2 – Operation modes of the dynamic (a) and louver (b) separation devices: a – dependence of the hydraulic resistance coefficient ζ on the flow velocity V for the dynamic separation device; b – dependence of the separation efficiency η on the flow velocity V for the louver (solid line) and dynamic (dashed line) separation devices

An essential parameter of the separation devices is hydraulic resistance. Its value depends on the coefficient of hydraulic resistance, which is determined experimentally [9]. The value of this parameter for louver separation devices can vary from 4 to 400 depending on the design [10, 11]. In turn, dynamic separation devices, in contrast to louvers, have a variable coefficient of hydraulic resistance ζ (depending on the flow velocity V). The primary trend of this dependence is shown in Figure 2 a. Mainly, as the velocity of the gas-liquid flow increases, the cross-sectional area increases too. Therefore, the coefficient of hydraulic resistance decreases.

The primary parameter in assessing the efficiency of a separation device is the degree of separation as the coefficient of separation efficiency. This parameter is the most commonly used as the amount of separated dispersed phase to its content in the gas-liquid mixture at the inlet to the separator. [12].

In traditional designs of louver separation devices, this parameter varies depending on the inlet velocity of the gas-liquid flow. The primary trend of this change is shown in Figure 2 b by solid line [13]. The higher the flow rate, the greater the inertia force acting on the droplet liquid, causing its separation. Therefore, efficiency increases.

On the other hand, the destruction of the droplets leads to a halt in the growth of separation efficiency (a horizontal line in Figure 2 b) at a specific flow rate.

The destruction of droplets is so essential that in combination with the film destruction for the already captured liquid (and consequently, secondary splashing) leads not only to stop the growth of efficiency but also to its sharp decrease [3, 14].

Unlike a louver separation device, avoiding a decrease in separation efficiency in a dynamic separation device can be accomplished by preventing a critical increase in the effective aerodynamic force as the velocity of the gas-

liquid flow increases. This occurs by increasing the cross-section of the channel. As a result, the range of effective operations is expanding. The primary trend for a dynamic separation device is indicated in Figure 2 b by a dashed line. Thus, the primary advantage of dynamic separation devices is working as an automatic control system. In this case, the object of regulation is the hydraulic resistance and the regulating action – elastic forces. Due to this, it is possible to maintain the degree of gas purification in a wide range of possible changes in the flow rate of the gas-liquid mixture. Therefore, increasing the efficiency of the separation of heterogeneous systems through vibration-inertial separation methods is an urgent problem. It is necessary to perform physical modeling of vibration-inertial separation processes to define the essential working characteristics of dynamic separation devices.

3 Research Methodology

3.1 General formulation

Regardless of their design, dynamic separation devices include elastic elements of different types (Figure 1). These elements can change their shape under the action of the gas flow hydrodynamics. The change in the cross-section influences the flow parameters. Therefore, aerohydroelastic phenomena occur.

For developing an engineering method to calculate separation devices, it is necessary to solve the problem of aerohydroelasticity separately, considering the features and appropriate simplifications and assumptions. Given that depending on the content of the liquid phase may change the nature of the interaction of gas-liquid flow and elastic elements, the solution of this problem can be divided into the following four stages [15].

The first stage is conducting full-scale and numerical experiments. It determines and compares the gas flow rate, which causes loss of static and dynamic stability of elastic elements. When the static stability is lost, the numerical experiment is verified using the values of the deviations of the elastic elements and the gas flow velocities that caused them. Due to the numerical experiment gives a better idea of the flow structure and the deflected mode of the elements, the pressure distribution depending on the velocity and deformation is determined. The data can be used to determine the stiffness of the elements and damping of the gas flow. Therefore, the mathematical model can be refined. Verification of a dynamic stability loss by conducting a numerical experiment using oscillation frequency and amplitude of elastic elements is carried out. From the verified numerical experiment, it is possible to determine the pressure distribution over the elastic elements as a function of time and flow rate, and as a consequence, the value of damping as a function of time.

The second stage is conducting experimental studies of the interaction of elastic elements and gas-liquid flow with different liquid phase concentrations. The loss of static and dynamic stability depending on the flow rate in a specific range of the content of the dispersed liquid in the gas flow is investigated. Verification of the numerical experiment is carried out similarly to the first stage and determines the pressure distribution on the elastic elements depending on the gas-liquid flow rate and the concentration of the liquid phase in case of loss of static stability and as a function of time in case of loss of dynamic stability. The obtained data are used to determine the stiffness of the elastic elements and the damping coefficients of the gas-liquid flow. Comparing the obtained data with the previous stage results, we can conclude about the effect of different concentrations on the stability of elastic elements, determine the separation efficiency, and consider the possibility of using vibrations for coagulation of droplets.

The third stage is studying the influence of mechanical oscillations of elastic elements on the gas-liquid flow. The expected effect is the coagulation of droplets, hence increasing their separation efficiency, similar to the effect of vibroacoustic coagulation. According to features of the specified effect, it is possible to observe both coagulation of drops and their destruction depending on a combination of the following parameters: gas-liquid flow rate, the oscillation frequency, and droplet dispersion.

Therefore, while studying the effect of mechanical oscillations on the flow, we have used a mathematical model, in which the identification was made with all the necessary parameters to find the size of the separation device. Such an approach increases the efficiency of separating the input gas-liquid mixture due to the coagulation of droplets. According to these dimensions, it is necessary to make a separation element to investigate the effect of oscillations.

The fourth stage is conducting a full-scale and numerical experiment to study the mutual effect of installed sequentially dynamic separation devices. Of particular interest is the change in the critical velocities of the gas-liquid flow (buffing and fluttering). These effects cause the phenomenon of dynamic instability, depending on the distance between the devices. The change in critical velocity may differ depending on the location in the gas flow.

Let us consider the features of researching each of the designs of the devices shown in Figure 1. The main differences are the different methods of their manufacture. For example, in a separation device where the elastic elements are truncated parabolic half-cylinders, the elastic elements (plates) are in a pre-deformed state. It must be considered since it affects their rigidity. The elastic elements have no internal stresses in the other two devices before the gas-liquid flow enters the separation channel. This is because in a dynamic device with four inputs, they are not deformed at all at the initial time. In the channel with sinusoidal walls, their shape is planned to be obtained using a vacuum press. Remarkably, one of the main difficulties in developing separation devices with elastic elements of sinusoidal shape is the choice of material. The mechanical properties of the material should provide the necessary deformations while holding the shape.

3.2 Experimental setup

Given the stages of scientific research described above, an experimental stand was developed (Figures 3, 4). It provides the solution to the following problems:

– to provide easy change of modular separation devices;

– to measure the deviation of elastic elements in the subcritical mode;

– to measure oscillation amplitudes and frequencies during the loss of dynamic stability;

– to measure the separation efficiency for a gas-liquid mixture and hydraulic resistance;

– to determine the effect of mechanical oscillations on the gas-liquid flow.

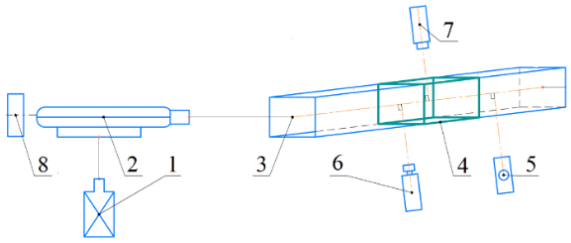

Figure 3 – The design scheme of the experimental stand:
1 – fog generator; 2 – centrifugal gas blower; 3 – test section;
4 – test model of the dynamic modular separation device;
5 – anemometer; 6 – high-speed camera; 7 – stroboscope;
8 – frequency regulator

a b

Figure 4 – Photo of test section (a) and frequency regulator (b)

Let us consider in detail the operation of the experimental stand, the design scheme of which is given in Figure 3 and the photo – in Figure 4. Dispersed liquid generated by the fog generator “Longray 2680A-II” 1 is fed to the centrifugal blower 2, where it mixes with the gas flow. Under the action of pressure, it is sent to the channel of the experimental stand, where the model of the modular dynamic separation device is installed. The deformation of an elastic element concerning the scale put on the channel walls is fixed using the high-speed camera. The camera is mounted on a tripod. The level gauge measures its position. In test section 3, the gas-liquid flow passes the modular dynamic separation device 4, where the capture of dispersed particles occurs. The captured film liquid is removed from the separator. The purified gas is released into the atmosphere. The airflow of the centrifugal blower is regulated by the frequency regulator “Aqua Drive FC 200”. The cold mist generator 1 allows us to adjust the dispersion of the liquid in a range from 5 to 50 μm. Therefore, the separation efficiency can be determined for different particle sizes.

Figure 4 a shows that the test section consists of two parts having a square cross-section of 125 mm × 125 mm and a length of 400 mm. Such geometric dimensions were selected to ensure uniformity of flow at the inlet of the modular dynamic separation device. For this purpose, the transition nozzle from a round cross-section to a square one is used as a diffuser with an angle of 15°. The elastic elements of the modular separation device are fixed between the two parts of the test section. This fastening was chosen to minimize the impact of the housing rigidity on the oscillations of the elastic elements when they lose dynamic stability. The elements specified in Figure 1 a without inclination are considered. Therefore, their shape is a parabolic half-cylinder. The length of the plates is 210 mm.

The procedure for conducting a physical experiment at the first stage of research is as follows. Firstly, the frequency regulator is switched on, and the rotation speed of the electric motor’s rotor connected to a centrifugal gas blower is exposed. An anemometer measures the flow rate at the inlet to the modular separation device. As a result, dependence between the velocity of the gas-liquid flow and the speed of the motor is built.

Secondly, the gas flow enters the test section, where a modular separation device is installed. If the gas flow does not cause loss of dynamic stability, they are measured using a scale on the body and are tabulated. If oscillations of the elastic elements occur, recording is performed for one minute using a high-speed camera with 240 frames per second shooting speed. After, the resulting video is decomposed into frames. Comparing every two adjacent frames allows us to measure the speed of the elastic elements and determine the oscillation frequency.

Thirdly, a series of experiments are performed for the thicknesses of elastic elements of 0.4, 0.5, and 0.6 mm for different values of gas flow rate, liquid volume fraction, and dispersion. Notably, in the case of the stability loss (at a particular input flow velocity), it is necessary to wait until the mode is set because a particular time is required for damping the oscillations.

After carrying out the measurements mentioned above, new plates are installed. In this case, the frequency is set on the frequency regulator, at which the velocity of the gas-liquid flow causes oscillations of the elastic elements. The obtained time allows us to investigate the fatigue strength of elastic elements, particularly the number of bends before their destruction.

Let us consider the difference between conducting experimental research in the first and second stages. At the first stage (switching on the gas blower), the fog generator is switched on. The dispersion of droplets is established, and the resulting mist is fed to the centrifugal blower. After, the deviation of elastic elements to the loss of stability is measured. Also, the velocity of their movement, the oscillation frequency, the critical flow velocity, and the time before the destruction of the elastic element are determined. The obtained results are tabulated and compared with the corresponding results of the first stage. Additionally, the separation efficiency before the stability loss is measured.

At the third stage of research, the separation efficiency after the loss of dynamic stability is measured. In this case, a series of experiments are performed for different combinations of fluid dispersion and oscillation frequency of elastic elements. The obtained results are tabulated too.

Fourthly, two modules of dynamic separation elements are installed in the housing. At this research stage, the fog generator does not switch on but only adjusts the speed of the blower's rotor. Studying is made on both modules, and the critical input velocity that causes oscillations is determined for each module.

Simultaneously, experimental studies were carried out within the research program and methodology developed according to DSTU 3974-2000 "System of Product Development and Launching into Manufacture".

4 Results

Experimental studies of elastic baffles with a thickness of 0.4, 0.5, and 0.6 mm and a length of 200 mm have been carried out to determine the gas flow rate, at which there is a loss of dynamic and static stability. The height of baffle elements corresponds to the height of the channel. Baffle elements are made from polyvinyl chloride with the following mechanical properties: Young's modulus 2.8 GPa; Poisson's ratio 0.385 [1].

The plates had no preliminary deformation before installing them in the channel. A thermoanemometer "Hot Wire Anemometer HT-9829" is used to determine the flow velocity. Velocity measurements were performed without the installation of elastic baffles in the channel.

After carrying out measurements, it is possible to allocate some modes of work of an elastic baffle element. The symbols indicated in Figure 5 were introduced to facilitate the analysis of the results.

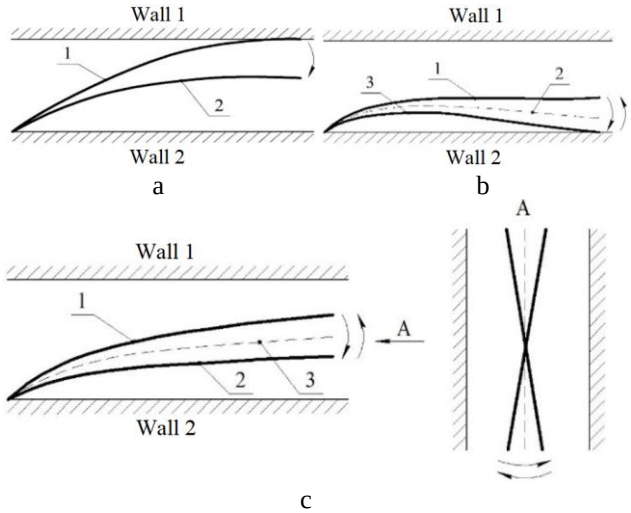

Figure 5 – Experimentally obtained operating modes for baffle element with thickness of 0.5 mm

There are no oscillations at the first mode (gas flow velocity is less than 4 m/s). Only a static deflection appears, as shown in Figure 5 a. In this case, at an inlet velocity of less than 2.2 m/s, the deviation of the element is not observed because the gas flow passes through the gaps between the upper and lower walls of the channel and the elastic baffle element.

At the second stage (velocity range of 4.0–7.4 m/s), oscillations of the baffle element occur. It touches the upper and lower walls due to the occurrence of bending and torsional oscillations, schematically shown in Figure 5 b. As a result, the oscillating plate approaches wall 2.

At the third stage (velocity range of 7.4–11.6 m/s), the element begins to touch wall 2 (Figure 5 c), including bending torsional oscillations. The speed of 11.6 m/s was taken as a limiting value when the elastic baffle element is pressed to wall 2 and stops moving.

Let us consider the dependence of each oscillation parameter on the gas flow velocity. Three functions have been used to describe the relationship between the deviation of the elastic element (or equilibrium position) A depending on the speed V in each of the three modes mentioned above.

Let us start with the first mode, in which there are static deviations from the starting position. It includes the first six points. A linear function is applied:

$$A = b_1 V + b_0. \quad (1)$$

We did not set element b_0 to zero because noticeable deviations appear at a velocity above 2.2 m/s. Before that, the gas flow passes over the upper and lower part of the plate.

The least-squares method was used to determine the regression coefficients:

$$F = \sum_{i=1}^{n} (A_1 - b_0 - b_1 \cdot V_i)^2 \to min. \quad (2)$$

Since the problem of determining the coefficients of a linear polynomial is reduced to finding the minimum of the function, we have equated to zero the partial derivatives with respect to the evaluated coefficients:

$$\begin{cases} \frac{\partial F}{\partial b_0} = -2 \cdot \sum_{i=1}^{n} (A_1 - b_0 - b_1 \cdot V_i) = 0, \\ \frac{\partial F}{\partial b_1} = -2 \cdot \sum_{i=1}^{n} (A_1 - b_0 - b_1 \cdot V_i) \cdot V_i = 0. \end{cases} \quad (3)$$

The transformation to obtain the resulting system of linear equations with two unknowns b_0 and b_1 are performed:

$$\begin{cases} b_0 \cdot n + b_1 \cdot \sum_{i=1}^{n} V_i = \sum_{i=1}^{n} A_i, \\ b_0 \cdot \sum_{i=1}^{n} V_i + b_1 \cdot \sum_{i=1}^{n} V_i^2 = \sum_{i=1}^{n} (V_i \cdot A_i). \end{cases} \quad (4)$$

The inverse matrix method is used to determine them:

$$\begin{pmatrix} b_0 \\ b_1 \end{pmatrix} = \begin{pmatrix} n & \sum_{i=1}^{n} V_i \\ \sum_{i=1}^{n} V_i & \sum_{i=1}^{n} V_i^2 \end{pmatrix}^{-1} \cdot \begin{pmatrix} \sum_{i=1}^{n} A_i \\ \sum_{i=1}^{n} (V_i \cdot A_i) \end{pmatrix}. \quad (5)$$

Therefore, the following regression coefficients were obtained using the computer algebra system "MahtCAD" for the first mode of operation: b_0 = –44.6, b_1 = 18.8. As a result, regression (1) takes the following form:

$$A = 18.8 \cdot V - 44.6. \quad (6)$$

Equating this equation to zero, the velocity at which deviations occur can be determined. Its value equals 2.4 m/s, which differs by 0.2 m/s from the experimentally obtained value of 2.2 m/s.

For linear polynomials, the correlation coefficient is used to quantify the closeness of the relationship between the quantities. Its value is equal to 0.98. According to the Chaddock scale, this value corresponds to a very high direct relationship between velocity and deviation.

In the oscillation modes of operation, the description of the equilibrium position depending on the gas velocity is described. The polynomial coefficients are determined using the least-squares method: $b_0 = -17.0$, and $b_1 = 12.2$. The resulting regression equation is as follows:

$$A = 12.2 \cdot V - 17.0. \quad (7)$$

The correlation coefficient is equal to 0.97. According to the Chaddock scale, this value corresponds to a very high direct relationship between speed and equilibrium.

Figure 6 presents the dependence of the plate's position on the velocity of the incoming gas flow. The vertical lines show the limits of the modes in the operation of the separation element described above.

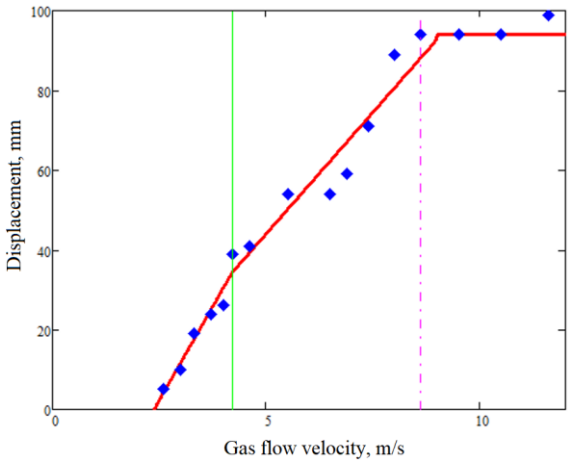

Figure 6 –Dependence of the plate's deflection on the gas flow velocity

The following parameter, the dependence of which was considered on the gas flow velocity V, is the amplitude of oscillations X. Notably, to describe the dependence on the second mode of operation (velocity range of 4.2–7.4 m/s), a polynomial of the second degree is used:

$$X = a_0 + a_1 \cdot V + a_2 \cdot V^2. \quad (8)$$

As for a linear polynomial, the determination of the unknown coefficients of a polynomial of the second degree can be performed using the least-squares method:

$$F = \sum_{i=1}^{n\Sigma}(X_i - a_0 - a_1 \cdot V - a_2 \cdot V^2)^2 \to min. \quad (9)$$

It is necessary to equate to zero three partial derivatives with respect to the coefficients a_0, a_1, and a_2:

$$\begin{aligned} \frac{\partial F}{\partial a_0} &= -2 \cdot \sum_{i=1}^{n}(X_i - a_0 - a_1 \cdot V_i - a_2 \cdot V_i^2) = 0, \\ \frac{\partial F}{\partial a_1} &= -2 \cdot \sum_{i=1}^{n}(X_i - a_0 - a_1 \cdot V_i - a_2 \cdot V_i^2) \cdot V_i = 0, \\ \frac{\partial F}{\partial a_2} &= -2 \cdot \sum_{i=1}^{n}(X_i - a_0 - a_1 \cdot V_i - a_2 \cdot V_i^2) \cdot V_i^2 = 0. \end{aligned} \quad (10)$$

In this case, when performing transformations, a system of linear equations with three unknowns a_0, a_1, and a_2 is obtained:

$$\begin{cases} a_0 \cdot n + a_1 \cdot \sum_{i=1}^{n} V_i + a_2 \cdot \sum_{i=1}^{n} V_i^2 = \sum_{i=1}^{n} X_i, \\ a_0 \cdot \sum_{i=1}^{n} V_i + a_1 \cdot \sum_{i=1}^{n} V_i^2 + a_2 \cdot \sum_{i=1}^{n} V_i^3 = \sum_{i=1}^{n}(X_i \cdot V_i), \\ a_0 \cdot \sum_{i=1}^{n} V_i^2 + a_1 \cdot \sum_{i=1}^{n} V_i^3 + a_2 \cdot \sum_{i=1}^{n} V_i^4 = \sum_{i=1}^{n}(X_i \cdot V_i^2). \end{cases} \quad (11)$$

Therefore, the solution of the above system using the inverse matrix method has the following form:

$$\begin{pmatrix} a_0 \\ a_1 \\ a_2 \end{pmatrix} = \begin{pmatrix} n & \sum_{i=1}^{n} V_i & \sum_{i=1}^{n} V_i^2 \\ \sum_{i=1}^{n} V_i & \sum_{i=1}^{n} V_i^2 & \sum_{i=1}^{n} V_i^3 \\ \sum_{i=1}^{n} V_i^2 & \sum_{i=1}^{n} V_i^3 & \sum_{i=1}^{n} V_i^4 \end{pmatrix}^{-1} \cdot \begin{pmatrix} \sum_{i=1}^{n} X_i \\ \sum_{i=1}^{n}(X_i \cdot V_i) \\ \sum_{i=1}^{n}(X_i \cdot V_i^2) \end{pmatrix}. \quad (12)$$

For the second mode of operation, using the computer algebra system "MahtCAD", the following values of regression coefficients were obtained: $a_0 = 121.2$, $a_1 = -39.8$, and $a_2 = 4.9$. The resulting regression equation (8) takes the following form:

$$X = 121.1 - 39.8 \cdot V + 4.9 \cdot V^2. \quad . \quad (13)$$

Fisher's criterion is used to verify the significance of the regression model.

Given that the number of explanatory variables is equal to 1, the number of degrees of freedom of the explained variance is also equal to 1. The number of degrees of freedom for unexplained variance is calculated depending on the number of experimental points and the number of explanatory variables. So, it is equal to $5 - 1 - 1 = 3$. Therefore, the obtained correlation coefficient is 0.999, and Fisher's criterion is $F = 1806$. The Fisher's criterion is defined according to the corresponding table for the accepted significance level 0.05 and the above-stated degrees of freedom. It is equal to $F_{tab} = 10.13$. Since the actual value $F > F_{tab}$, the regression equation (13) is statistically reliable.

At the next stage (velocity range of 7.4–11.6 m/s), the relationship between the oscillation amplitude and the gas flow velocity was carried out using a polynomial of the second degree too, with the determination of its coefficients by the least-square method. The resulting dependence takes the following form:

$$X = 286.2 - 41.5 \cdot V + 1.9 \cdot V^2. \quad (14)$$

As in the previous case, we evaluated the accuracy of the relationship between the amplitude and the gas flow velocity using Fisher's criterion. In this case, the number of degrees of freedom for unexplained variance is equal to 5. The correlation coefficient is 0.902, Fisher's criterion $F = 21.9$, and its table value $F_{tab} = 6.61$. Therefore, the regression equation (14) is also statistically reliable.

The obtained relationships between the gas flow velocity and the oscillation amplitude for both operation modes are shown in Figure 7. Vertical lines indicate the boundaries of these modes.

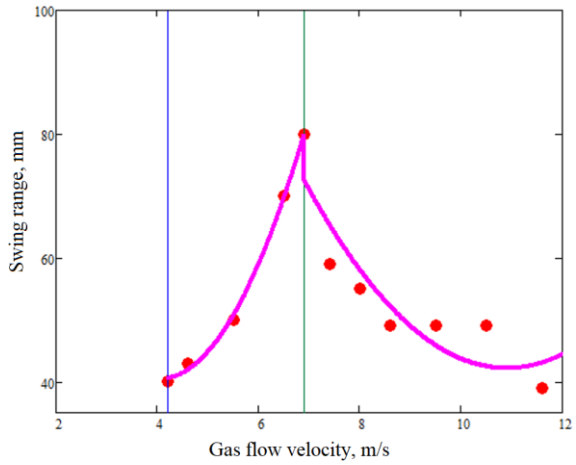

Figure 7 – Dependence of the swing range on the inlet gas flow velocity

The last parameter of oscillations studied during the experiment is the oscillation frequency. To estimate its change from increasing speed, we have found the percentage of its minimum value from the maximum. For the data obtained at the first stage of research, it is equal to 96.7 %. This parameter in the studied speed range does not change significantly. Therefore, the frequency can be considered constant when using a dynamic separation element for vibrocoagulation of droplets.

Additionally, the frequency and amplitude of the elastic baffle element with a thickness of 0.4 mm were measured. The least-squares method was used to process the results of the experiment. There are three operation modes, as in the case of a baffle element with a thickness of 0.5 mm.

Let us consider the operation of an elastic baffle element with a thickness of 0.6 mm in more detail. Its feature is the presence of four operation modes (Figure 8), differing from the plates with 0.4 and 0.5 mm thickness.

At the first stage (velocity range of 3.3–4.8 m/s), the oscillations of the baffle element occur. It does not touch any wall of the channel, which is schematically shown in Figure 8 a. Необхідно відмітити, що при швидкості входу меншій за 3.3 m/s відхилення елементу не спостерігаються, а у випадку їх виникнення являються надто малими для вимірювання.

At the second stage (velocity range of 4.8–6.6 m/s), oscillations of the elastic baffle element continue. In this case, the element begins to touch wall 1, as shown in Figure 8 b. The element's position is close to wall 2; touches occur by increasing the amplitude of oscillations.

At the third stage (velocity range of 6.6–9.9 m/s), bending-torsional oscillations occur, as evidenced by touching the upper and lower walls of the channel. Since the element's position approached with increasing speed to wall 2, the element stopped touching wall 1. This operation mode is schematically shown in Figure 8 c.

At the fourth mode (velocity range of 9.9–13.1 m/s), the element touches wall 2. In this case, bending-torsional oscillations continue (Figure 8 d).

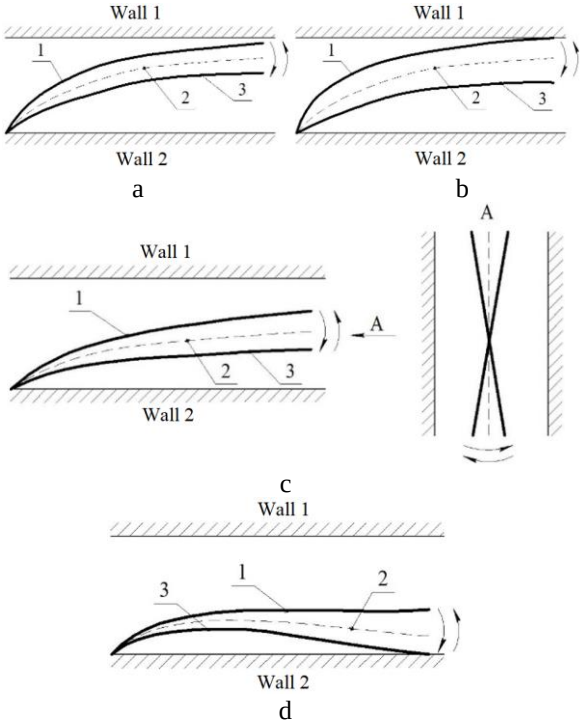

Figure 8 – Operating modes of the baffle element with the thickness of 0.6 mm: 1 – small displacements; 2 – large displacements; 3 – position of equilibrium

Notably, the gas flow velocity of 13.1 m/s is the maximum one while studying this design.

The obtained results were analyzed using the least-square method to find the coefficients of polynomials of the first and second degrees, describing the relationship between the amplitude of oscillations, the position of the elastic baffle element, and the velocity of the gas flow.

As a result, the graph of the plate's position on the velocity of the incoming gas flow is built in Figure 9.

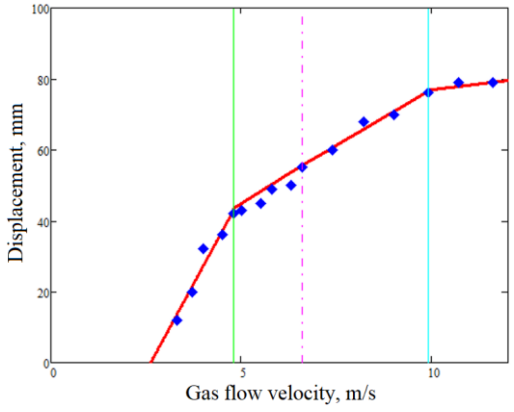

Figure 9 – Dependence of the plate's position on the gas flow velocity

Vertical lines show the mode boundaries. At the fourth mode, it should be noted that the line (as in previous cases) is almost horizontal.

Let us consider in more detail the obtained graph of the dependence of the amplitude of the elastic baffle element on the speed of the oncoming gas flow (Figure 10).

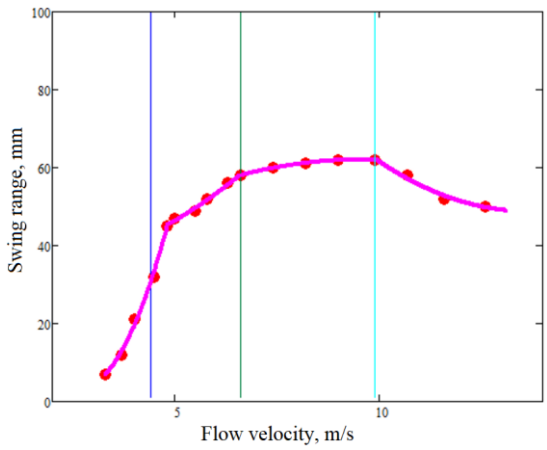

Figure 10 – Dependence of the swing range on the inlet flow velocity

In the operating modes of the separation element, in which there is no contact with the wall of channel 2, the dependence of the amplitude of oscillations on the flow velocity is increasing. In the last mode, it decreases, as in all previous cases. It should be noted that in the third mode, the dependence is almost linear, given the coefficient near the variable squared.

The percentage of the elastic baffle element's minimum and the maximum oscillation frequency is 78.8%, which may affect the coagulation of droplets.

An alternative material, ABS plastic, was proposed to manufacture elastic baffles with a thickness of 0.4 mm. This material has the following mechanical properties: Young's modulus 1.7 GPa, and Poisson's ratio 0.30. As in the case of elastic baffles made of polyvinyl chloride with a thickness of 0.4 and 0.5 mm, the operation of the above elements from ABS plastic can be divided into similar three modes.

5 Discussion

As can be seen from the results of experimental studies, the operation of the separation element from ABS plastic has a few features, mainly as follows. A wide first operating mode (коливання відсутні): velocity range of 1.1–5.3 m/s. In the first mode, there are significant deviations of the elastic element: 15–60 mm. A narrow second operating mode: velocity range of 5.5–6.3 m/s. A wide third operating mode (the element performs torsional oscillations while touching the wall 2): velocity range of 6.3–11.6 m/s. Notably, the operation is limited by the gas flow velocity of 11.8 m/s, at which the element under the action of the flow is pressed against wall 2. Thus, the regression equations for the dependence of various parameters on the flow rate were obtained. For a plate with a thickness of 0.4 mm from polyvinyl chloride, the regression equation for the deviation on the gas flow velocity is as follows: $A = 10.6V - 1.0$. The regression equation for the dependence of the equilibrium position on the velocity is as follows: $A = 6.1V - 24.0$.

In the second operating mode, the regression equation for the dependence of the swing range on the speed is as follows: $X = 36.1 - 6.9V + 6.9V^2$. Fisher's criterion calculated on the given mode takes $F = 53$ compared to tabular value $F_{tab} = 18.51$. In the third operating mode, the regression equation for the dependence of the swing range on the speed is as follows: $X = 666.2 - 118.9V + 5.8V^2$. Fisher's criterion calculated on the given mode takes $F = 6337$ compared to tabular value $F_{tab} = 6.61$.

6 Conclusions

The paper considers dynamic separation devices that operate as automatic control systems. Due to this, they allow increasing the efficiency of the separation process in heterogeneous systems. The method of conducting physical experiments of these devices and experimental setup for their study are presented.

As a result of experimental research, the operation modes of separation devices were determined for different plate thicknesses, i.e., 0.4, 0.5, and 0.6 mm. The obtained dependencies of the plate's position on the oncoming gas flow velocity and the oscillation amplitudes on different operation modes have been estimated.

The following regression equations for different parameters of flow rate were also obtained. E.g., for a plate of 0.4 mm thick from polyvinyl chloride, deviation, the position of equilibrium, and swing range on the 2nd and 3rd modes have been obtained. Fisher's criteria confirm the adequacy of the proposed model.

The obtained results verify the mathematical model and substantiate the primary parameters of studied separation devices.

7 Acknowledgments

The developed methodology was realized within the research project "Creation of new granular materials for nuclear fuel and catalysts in the active hydrodynamic environment" (State reg. No. 0120U102036). The authors also appreciate the support of the International Association for Technological Development and Innovations.

References

1. Shah, S., Koralewicz, P., Gevorgian, V., Liu, H., Fu, J. (2021). Impedance methods for analyzing stability impacts of inverter-based resources: Stability analysis tools for modern power systems. *IEEE Electrification Magazine*, Vol. 9(1), pp. 53–65.
2. Sujan, S., Jamal, M., Hossain, M., Khanam, M., Ismail, M. (2015). Analysis of gas condensate and its different fractions of Bibiyana gas field to produce valuable products. *Bangladesh Journal of Scientific and Industrial Research*, Vol. 50(1), 59.
3. Liaposhchenko, O. O., Sklabinskyi, V. I., Zavialov, V. L., Pavlenko, I. V., Nastenko, O. V., Demianenko, M. M. (2017). Appliance of inertial gas-dynamic separation of gas-dispersion flows in the curvilinear convergent-divergent channels for compressor equipment reliability improvement. *IOP Conference Series: Materials Science and Engineering*, Vol. 233(1), 012025.
4. Eremenko, O., Novikova, A. (2019). Improvement of technologies as a basis for effective development of mature field. *Tyumen 2019: 6th Conference*, Vol. 2019, pp. 1–5, doi: 10.3997/2214-4609.201900625.
5. Stewart, M., Arnold, K. (2008). Two-phase gas-liquid separators. Gas-liquid and liquid-liquid separators. *In: Stewart, M., Arnold, K. (Eds.) Gas-Liquid And Liquid-Liquid Separators. Gulf Professional Publishing*, pp. 65–130.
6. Gaile, A. A., Chistyakov, V. N., Koldobskaya, L. L., Kolesov, V. V. (2012). Extraction purification of light gas oils of secondary oil refining processes. *Chemistry and Technology of Fuels and Oils*, Vol. 48(3), pp. 187–194, doi: 10.1007/s10553-012-0357-9.
7. Liaposhchenko, O. O., Pavlenko, I. V., Nastenko, O. V., Usyk, P. Yu., Demianenko, M. M. (2015). *Method of Capturing Highly Dispersed Droplet Liquid from Gas-Liquid Stream*. Patent of Ukraine, 102445 U, B01D 45/04 (2006.01), Sumy State University.
8. Liaposhchenko, O. O., Nastenko, O. V., Pavlenko, I. V., et al. (2016). *Method of Capturing Highly Dispersed Droplet Liquid from Gas-Liquid Stream*. Patent of Ukraine, 111039 U, B01D 45/00 (2006.01), Sumy State University.
9. Kohl, A. L., Nielsen, R. (1997). *Gas Purification*. Elsevier, Amsterdam, Netherlands.
10. Fang, C., Zou, R., Luo, G., Ji, Q., Sun, R., Hu, H., Li, X., Yao, H. (2021). CFD simulation design and optimization of a novel zigzag wave-plate mist eliminator with perforated plate. *Applied Thermal Engineering*, Vol. 184, 116212.
11. Luan, Y., Sun, H. (2010). Application of numerical simulation in the design of wire-mesh mist eliminator. *2010 International Conference On Computer Design and Applications*, pp. 5-95–5-98, doi: 10.1109/iccda.2010.5540870.
12. Perry, R. H., Green, D. W. (2007). *Perry's Chemical Engineers' Handbook*. McGraw-Hill, New York, NY, USA.
13. Kharoua, N., Khezzar, L., Nemouchi, Z. (2010). Hydrocyclones for deoiling applications – A review. *Petroleum Science and Technology*, Vol. 28(7), pp. 738–755, doi: 10.1080/10916460902804721.
14. Vaidya, M. M., Duval, S., Hamad, F., O'Connell, J., Ghulam, S., Al-Talib, A., Bahamdan, A. A., Al-Otaibi, F. D. (2020). Improving the operation of split-flow sulfur recovery plants with membrane technology. *The Society of Petroleum Engineers - Abu Dhabi International Petroleum Exhibition and Conference 2020, ADIP 2020*, 165204.
15. Demianenko, M., Liaposhchenko, O., Pavlenko, I., Luscinski, S., Ivanov, V. (2020). Methodology of experimental research of aeroelastic interaction between two-phase flow and deflecting elements for modular separation devices. *Advanced Manufacturing Processes. InterPartner 2019. Lecture Notes in Mechanical Engineering. Springer, Cham*, pp. 489–499.